AD-A189 801 STUDY OF THE ENERGY TRANSFER MECHANISMS BETWEEN O2(1 DELTA) AND IODINE MONOFLUORIDE(U) AIR FORCE INST OF TECH WRIGHT-PATTERSON AFB OH SCHOOL OF ENGI 1/1

UNCLASSIFIED R O JOHNSON DEC 87 AFIT/GE/ENG/87D-27 F/G 7/2 NL

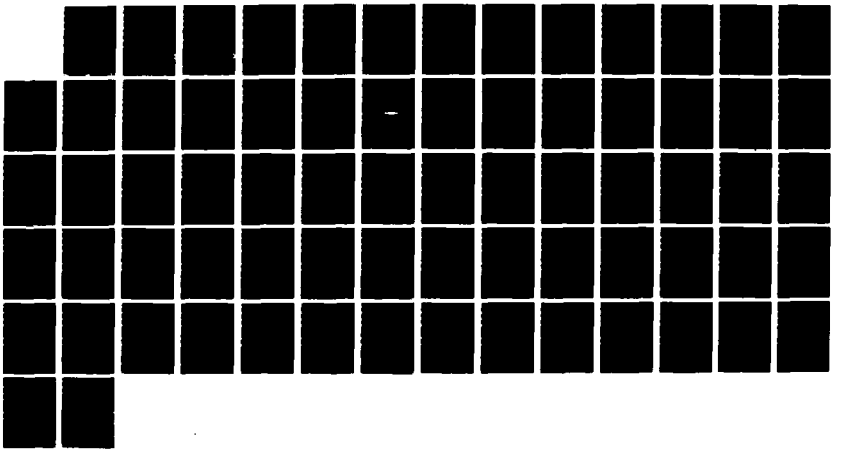

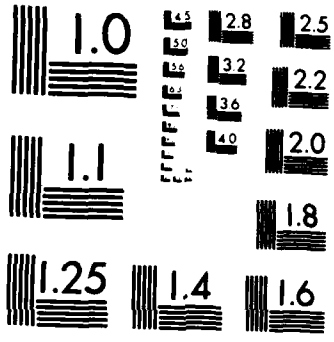

MICROCOPY RESOLUTION TEST CHART
NATIONAL BUREAU OF STANDARDS-1963-A

STUDY OF THE ENERGY TRANSFER MECHANISMS BETWEEN $O_2(^1\Delta)$ AND IODINE MONOFLUORIDE

THESIS

Ray O. Johnson
First Lieutenant, USAF

AFIT/GE/ENG/87D-27

DEPARTMENT OF THE AIR FORCE
AIR UNIVERSITY
AIR FORCE INSTITUTE OF TECHNOLOGY

Wright-Patterson Air Force Base, Ohio

AFIT/GE/ENG/87D-27

STUDY OF THE ENERGY TRANSFER MECHANISMS BETWEEN $O_2(^1\Delta)$ AND IODINE MONOFLUORIDE

THESIS

Ray O. Johnson
First Lieutenant, USAF

AFIT/GE/ENG/87D-27

AFIT/GE/ENG/87D-27

STUDY OF THE ENERGY TRANSFER MECHANISMS BETWEEN $O_2(^1\Delta)$ AND IODINE MONOFLUORIDE

THESIS

Presented to the Faculty of the School of Engineering

of the Air Force Institute of Technology

Air University

In Partial Fulfillment of the

Requirements for the Degree of

Master of Science in Electrical Engineering

Ray O. Johnson, B.S.

First Lieutenant, USAF

December 1987

Preface

This research is part of an on-going project at AFIT to better understand the energy transfer mechanisms involved in the oxygen and interhalogen molecule interaction. This understanding is achieved by using a flow tube reactor to characterize the chemiluminescence of various chemical substances, in this case oxygen and iodine monofluoride.

I found this work especially challenging because it was outside of the mainstream of my course work. I learned much theory and experienced the frustration and excitement that come with laboratory work. I was glad to be a part of this on-going AFIT endeavor.

I wish to thank Dr. Won B. Roh, my advisor, for the continuing guidance and support that he gave me during this effort; the study could not have been completed without his help. I also thank Dr. Ernest A. Dorko, at the Weapons Lab, who sponsored this thesis work. His expert knowledge of chemical lasers and flow-tube systems was invaluable. Additionally, this project could not have been completed without the work done by Tim Hancock and others at the AFIT Machine Shop who machined many parts for the flow tube reactor. Finally, I wish to thank my wife for her support and understanding during the last 18 months.

Ray O. Johnson

Table of Contents

List of Figures

List of Tables

Abstract

Chemiluminescence from the reaction between iodine monofluoride (IF) and oxygen has been observed in a flow tube reactor. Molecular oxygen in the singlet delta, first electronic excited state, $O_2(^1\Delta)$, has been used as the transfer agent. The IF($X \longrightarrow B$) transition requires 19054 cm^{-1} of energy, and $O_2(^1\Delta)$ can only supply 7918 cm^{-1} of energy in the transition to the ground state, $O_2(^3\Sigma)$. Despite the energy imbalance, $O_2(^1\Delta)$ is an efficient pump for IF. The kinetic mechanisms for this reaction are not well understood. The spectrum obtained from this emission has been compared to a known IF($B \longrightarrow X$) spectrum, and transitions have been assigned. A study of the emission intensity as a function of the $O_2(^1\Delta)$ concentration has been made. From the slope of the lines produced from the data, a possible reaction mechanism has been identified.

STUDY OF THE ENERGY TRANSFER MECHANISMS BETWEEN $O_2(^1\Delta)$ AND IODINE MONOFLUORIDE

I. Introduction

Background

An important group of substances known as halogens (X_2) or interhalogens (XY) consist of atoms or molecules made up of fluorine, chlorine, bromine, or iodine. These species have been found to make good active media in chemical lasers. Currently, iodine monofluoride (IF) is an important lasant candidate. The Air Force is interested in new lasants to support the development of Chemical Electronic Transition Laser (CETL) systems. These chemical systems are attractive because they do not require large electrical power supplies (12:1).

In order to increase the laser power output, an energy transfer agent is required to produce a substantial population inversion. Excited molecular oxygen in the singlet delta state, $O_2(^1\Delta)$, acts as the transfer agent by chemically pumping the lasant to a higher energy state. Although $O_2(^1\Delta)$ is an efficient energy transfer agent for halogens and interhalogens, the exact details of the energy transfer processes are not well understood.

In a system where IF is the lasant and $O_2(^1\Delta)$ is the transfer agent, IF is pumped from the ground state, IF(X), to the electronically excited B state, IF(B). This transition requires the input of 19054 cm^{-1} of energy (1:2243). However, $O_2(^1\Delta)$ can only supply 7918.1 cm^{-1} of energy in the transition to the ground state, $O_2(^1\Sigma)$ (14:85). It is seen though that $O_2(^1\Delta)$ is an efficient pump for IF (16:6793). It is unclear by what mechanism the lasant is raised to the necessary energy level.

Problem

The mechanisms by which $O_2(^1\Delta)$ excites IF from the ground to the excited B state are not well understood. The objective of this research is to determine, by means of a flow tube reactor and kinetic analysis, the reactions between $O_2(^1\Delta)$ and IF(X) which form IF(B).

Summary of Current Knowledge

Whitefield, Shea, and Davis studied the chemiluminescence produced by the interaction between IF and $O_2(^1\Delta)$ in experiments with a flow tube reactor (16:6794).

The Whitefield research group investigated three possible chemical reactions responsible for the emission from the IF(B) to IF(X) transition. Two of the three reactions which utilized $O_2(^1\Delta)$ produced much higher chemiluminescent intensities than the reaction without the singlet delta oxygen (16:6793). This strong dependence of the chemiluminescent intensity of the emission on the

excited oxygen species indicates the oxygen's importance in the production of IF(B) (16:6797).

The Whitefield group discussed the possible mechanisms of the reactions by using chemical kinetic analysis. Preliminary evidence indicated that $O_2(^1\Delta)$ may be a possible excitation source if sequential pumping is allowed. The sequential pumping requires intermediate states for the IF as it is pumped to the IF(B) state (16:6797).

The most recent research in IF chemical lasers was performed by Davis and others who were on contract with the United States Air Force Weapons Laboratory, Kirtland AFB, New Mexico. The team began their work by looking at ways of exciting IF by using metastable $O_2(^1\Delta)$ as a chemical laser pumping source (3:2).

The Davis team produced three quarterly status reports documenting their work for the Weapons Laboratory. Each report is reviewed below.

Report One. Initially, Davis and the research team looked for a mechanism by which O_2 could transfer the approximate 21100 cm^{-1} of energy needed to raise IF(X) to the IF(B; $v'>0$), excited state. The team postulated that since neither $O_2(^1\Delta)$ nor $O_2(^1\Sigma)$ had sufficient energy to directly pump IF(X; $v''=0$) to IF(B), sequential collisions must have been required. Sequential collisions require an energy reservoir in the IF manifold. The group found the two most likely candidates for the intermediate energy reservoir to be IF(X; $v'' >>0$) and IF($A'(^3\Pi_2)$) (3:2).

The research team reported that although $O_2(^1\Delta)$ cannot directly promote IF(X; v=0) to the A′ state, it appears that $O_2(^1\Sigma)$ may contain enough energy to populate the IF(A′) state (3:3). The team noted that the efficiency of IF(B) production could greatly depend on the rate of IF(A′) formation. The IF(A′) formation rate directly depends on whether $O_2(^1\Delta)$ or $O_2(^1\Sigma)$ molecules are involved in the energy transfer process (3:4). Several experiments were designed to determine the most efficient IF(B) formation.

The Davis team used a flow tube reactor to observe and measure the chemiluminescence produced by various experiments in order to understand the governing reactions. To vary the reactant's concentrations (control the experiment), the team added a quencher gas of either H_2 or CO_2 to quench $O_2(^1\Sigma)$, and the chemiluminescence intensities of both the $O_2(b \rightarrow X)$ and IF($B \rightarrow X$) were observed as a function of the added gas (3:8).

The results of the quenching studies indicated that $O_2(^1\Sigma)$ was directly involved in pumping IF(X) as expected, but the researchers felt that there was a second mechanism which produced much greater concentrations of IF(B) (3:14).

Report Two. In their second quarterly report, Davis and the research team made good progress in identifying the mechanisms involved in IF(B) excitation by $O_2(^1\Delta)$ (4:1).

From their work during the second reporting period, the team found that IF(B) was excited by two distinct processes.

Cold IF(X) was definitely pumped to IF(A') by $O_2(^1\Sigma)$ with a linear dependence of the concentrations (4:17). More importantly though, the team observed a second mechanism responsible for producing approximately two orders of magnitude more IF(B) than the $O_2(^1\Sigma)$. This second mechanism seems to involve sequential pumping of IF(B) via two separate reactions (4:17).

The quadratic dependency and the increased concentration of IF(B) indicate chemical efficiency, and are important if IF is to be used as a reactant in a chemical laser.

Report Three. During the third, and final, reporting period, the Davis research team concentrated their efforts on laser induced fluorescence studies of the IF(X,v) distribution resulting from an ICl + F reaction. These studies were used to help determine the role of IF(X) vibrational excitation in the O_2^* pumping process (5:10).

Limitations

This thesis will study reactions involving IF and $O_2(^1\Delta)$. A complete kinetic analysis of the reactions will not be given, but the reaction responsible for the excitation of IF from the ground to excited state will be determined. Because the experiment is to be performed in a laboratory, ideal environmental conditions are assumed.

Approach

An experiment will be performed using a chemical flow tube reactor, photomultiplier tube (PMT), and monochromator that will help experimentally verify theoretical postulates. Chemiluminescence, which will result from spontaneous emission, will be passed through a 0.3 meter monochromator and resolved into its component wavelengths. The resolved spectrum will be compared with the known spectrum of IF(B), and a study of the emission intensity as a function of the $O_2(^1\Delta)$ concentration will be made. From this data, the mechanism of the IF and oxygen interaction will be deduced by means of kinetic analysis.

II. Theory

Introduction

This section first presents a discussion of iodine monofluoride (IF) and oxygen spectroscopy, with emphasis on their applications to this experiment. Included is a brief discussion of oxygen in the singlet delta exited state, $O_2(a^1\Delta)$, which is an important component of this experiment. Finally, the theory of chemical kinetics as it relates to three proposed reactions in this experiment will be presented.

Spectroscopy of Iodine Monofluoride and Oxygen

Spectroscopy is the study of the absorption, emission, and scattering of electromagnetic radiation as related to the wavelength of the radiation. Molecular spectroscopy is the study of the interaction of electromagnetic radiation caused by molecules.

Molecular spectra are generally more complicated than atomic spectra, but even so, their properties can uniquely identify the molecule under study. The motion of the molecule indicates that the molecule contains a finite amount of energy. This energy is quantized according to the rules of quantum mechanics. Since IF is a diatomic molecule, the following discussions will be limited to diatomic molecules.

As a first approximation, the energy of a molecule can be represented as the sum of the electronic, vibrational, and rotational energies as shown in eq (2.1):

$$E = E_e + E_v + E_r \qquad (2.1)$$

Figure (2.1) shows the different vibrational and rotational levels between two electronic states of a molecule. The electronic states are shown as A and B, the vibrational levels are shown as v" and v', and the rotational levels are depicted by J'' and J'.

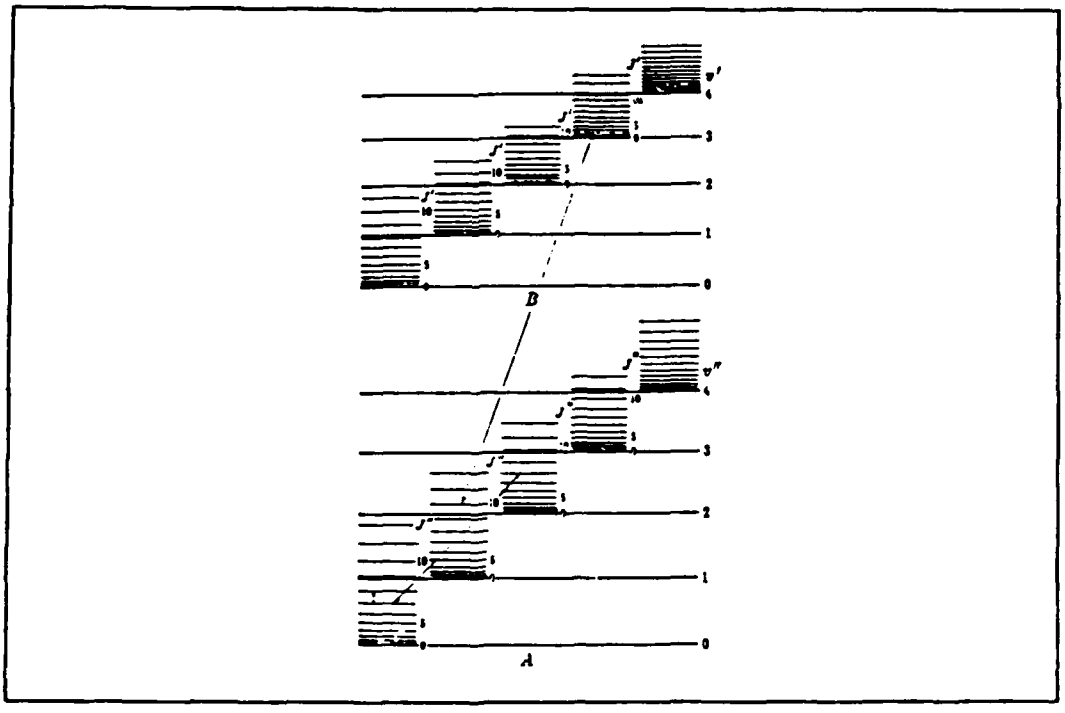

Figure 2.1. Energy Level Diagram of Two Electronic States (9:17)

The electronic energy of a molecule consists of kinetic and potential energy. The kinetic energy is present because the electrons have motion, and the potential energy originates because of mutual coulombic forces between the electrons and coulombic forces between the electrons and the atomic nuclei.

Electronic energy levels are the most widely separated levels, and when a transition occurs between electronic levels, the emitted photon is in the visible or ultraviolet spectrum.

The vibrational energy of a molecule arises due to the back-and-forth vibrational motion of the atoms. As a first approximation, the vibrations of a diatomic molecule can be represented as a harmonic oscillator. The energy levels of the harmonic oscillator are given below (9:21):

$$E_v = h\nu_{osc} (v + 1/2) \qquad (2.2)$$

where

E_v = vibrational energy (J)

h = Planck constant (J s)

ν_{osc} = oscillator frequency (Hz)

v = vibrational quantum number

Eq (2.2) is the solution to an eigenvalue equation which represents the energy of the harmonic oscillator. Eigenvalue equations have the property that operating on the

function regenerates the same function times a constant. The function that satisfies this equation is called the eigenfunction of the operator. The constant is called the eigenvalue associated with the eigenfunction (10:21). The eigenfunctions of the harmonic oscillator are Hermite polynomials, which are orthogonal functions (9:22).

Actually, the molecule is not best modeled by a harmonic oscillator but by an anharmonic oscillator. Instead of the potential function being a parabola, it is a curve as shown in Figure (2.2).

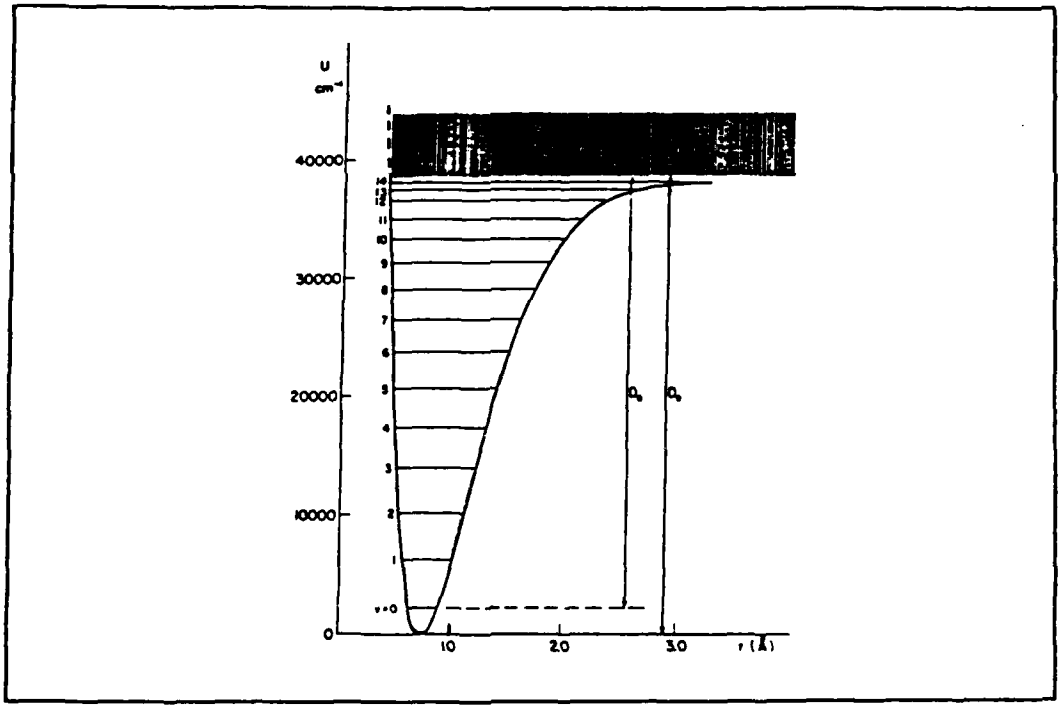

Figure 2.2. Potential Function and Vibrational Energy Levels of an Anharmonic Oscillator

The eigenfunctions of the anharmonic oscillator are similar to those of the harmonic oscillator, but are slightly distorted (9:25). Instead of the vibrational energy levels being equally spaced as in a harmonic oscillator, the separation between levels decreases as the vibrational quantum number increases, and the number of possible energy levels is finite. The levels converge as the vibrational quantum number increases, and eventually the force holding the atoms together is broken and the constituent atoms are separated. This separation is called dissociation.

Note that the energy of the lowest vibrational level is not zero, but has a finite amount of energy. Radiation between vibrational levels of a specific electronic level is in the mid infrared region.

A molecule's rotational energy occurs because the molecule rotates about its center of mass. The simplest model of the rotation of a diatomic molecule is the dumbbell model of two point masses connected by a massless rod (9:18). The rotational energy levels are given below (9:19):

$$E_r = \frac{h^2}{8\pi^2 I} J(J + 1) \qquad (2.3)$$

where

E_r = rotational energy (J)

h = Planck constant (J s)

I = moment of inertia (kg m^2)

J = rotational quantum number

For each of the energy values (eigenvalues) of the wave equation there is a corresponding characteristic function (eigenfunction) whose square gives the probability distribution function for the rotator (9:19).

Radiation between rotational energy levels in a certain electronic and rotational level are in the far infrared or microwave region of the spectrum. It is seen that changes in smaller energy terms usually accompany changes in larger energy terms. That is, absorption of ultraviolet or visible light will normally change the vibrational and rotational energies as well as the electronic energy.

As previously stated, the energies of a molecule are quantized according to the rules of quantum mechanics. That is, the molecule is only allowed to possess certain values of electronic, vibrational, and rotational energy.

When a molecule is exposed to radiation, it will undergo a transition from one energy level to another if the energy of the radiation matches the energy difference between the initial and some final energy level in the molecule. Energy level transitions also follow selection rules which further restrict the possible energy changes.

Although there are exceptions, the following selection rules are generally followed:

-- Rotational transitions

$$\Delta J = 0, +1, -1$$

-- Vibrational transitions within the same electronic state

$$\Delta v = \pm 1$$

-- Rotational transitions within the same vibrational state

$$\Delta J = \pm 1$$

In an atom, the electron is characterized by the quantum numbers n and ℓ, the principal and orbital angular quantum numbers. The symbol $\underline{l}$ is used to express the orbital angular momentum vector and ℓ for the corresponding quantum number. The magnitude of $\underline{l}$ is defined below (9:26):

$$\underline{l} = (\ell(\ell + 1))^{1/2} \left[\frac{h}{2\pi}\right] \simeq \ell \left[\frac{h}{2\pi}\right] \qquad (2.4)$$

In a molecule, where an electric field exists between the nuclei, the orbital angular momentum vector $\underline{l}$ can only have orientations for which the axial field component is $m_\ell(h/2\pi)$, where $m_\ell = \ell, \ell-1, \ell-2, \ldots, -\ell$. To distinguish the states of an electron with the same n and ℓ but different $|m_\ell|$, the greek letter lambda, λ, is used as defined below (9:25):

$$\lambda = |m_\ell| = \ell, \ \ell-1, \ \ldots, 0 \qquad (2.5)$$

As a shorthand method of indicating the orbital wave functions of one-electron states with $\lambda = 0, 1, 2, \ldots$, the symbols σ, π, and δ are used (9:26).

In a many-electron molecular system, each electron can roughly be considered separately, and each electron carries its own quantum numbers n_i, ℓ_i, and λ_i. For a given electron configuration, we obtain at least one electronic state. Each state is characterized by a total orbital angular momentum Λ, which is related to λ by the following equation (9:30):

$$\Lambda = \sum \lambda_i \qquad (2.6)$$

Again, the $\Lambda = 0, 1, 2, \ldots$, are denoted by the greek letters Σ, Π, Δ, ..., for ease of writing the states.

Another quantum number, m_s, the spin quantum number is also used to determine the spin state of the electron. The spin quantum number can have values $\pm 1/2$. The spins s_i of the individual electrons are added vectorially to yield the resultant spin, S, for the molecule, as shown below (9:30):

$$S = \sum s_i \qquad (2.7)$$

S also determines the multiplicity, or number of components, of the state. The multiplicity, $2S + 1$, is denoted by a left superscript above the term symbol, as $^3\Pi$. When S equals zero, the multiplicity is 1, and a singlet state is formed. When S equals one, a triplet state is formed (9:30).

For a given molecule there are a set of molecular orbitals, and for the molecule's lowest energy state, called the ground state, electrons occupy the lowest energy molecular orbitals. According to the Pauli exclusion principle, only two electrons can occupy a single orbital, and only if they have opposite spins. No two electrons are allowed to have the same four quantum numbers.

The ground state is the natural state of the molecule, but a higher energy state called an excited state can be achieved by absorption of radiation or by a collision. The molecular ground state is called the X state, and excited states are called the A, B, C, ... states or the a, b, c, ... states, where the capital letters indicate states with like multiplicities and small letters indicate states with differing multiplicities. Figure (2.3) is a potential energy curve for oxygen that shows the ground and excited states for the oxygen molecule. Figure (2.4) is a potential energy curve for the IF molecule.

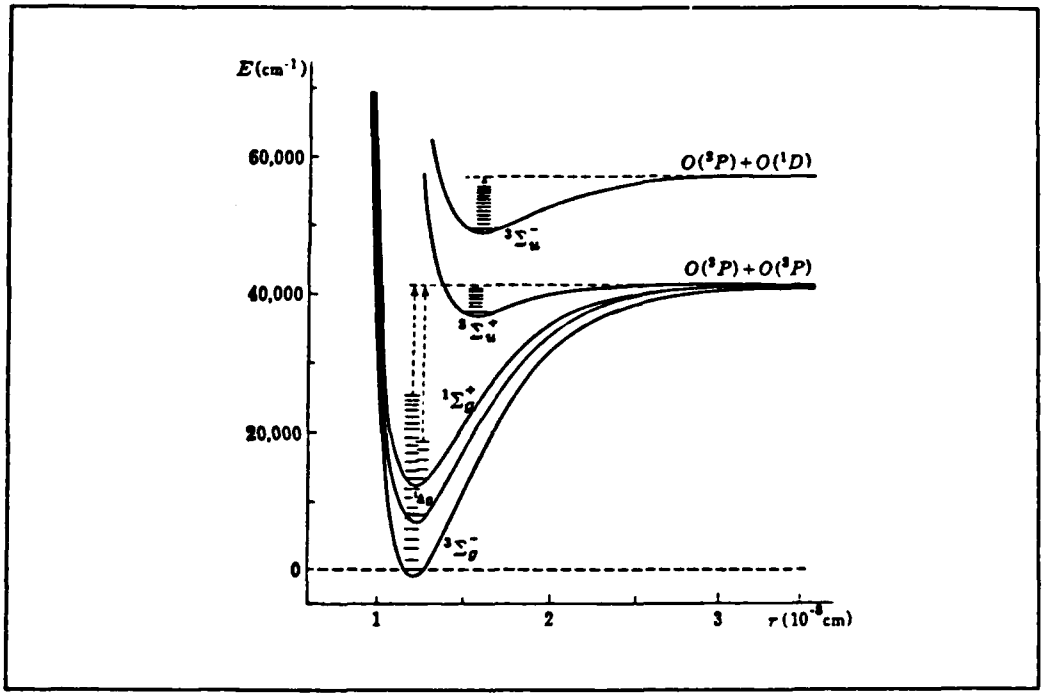

Figure 2.3. Potential Energy Diagram of Oxygen (8:446)

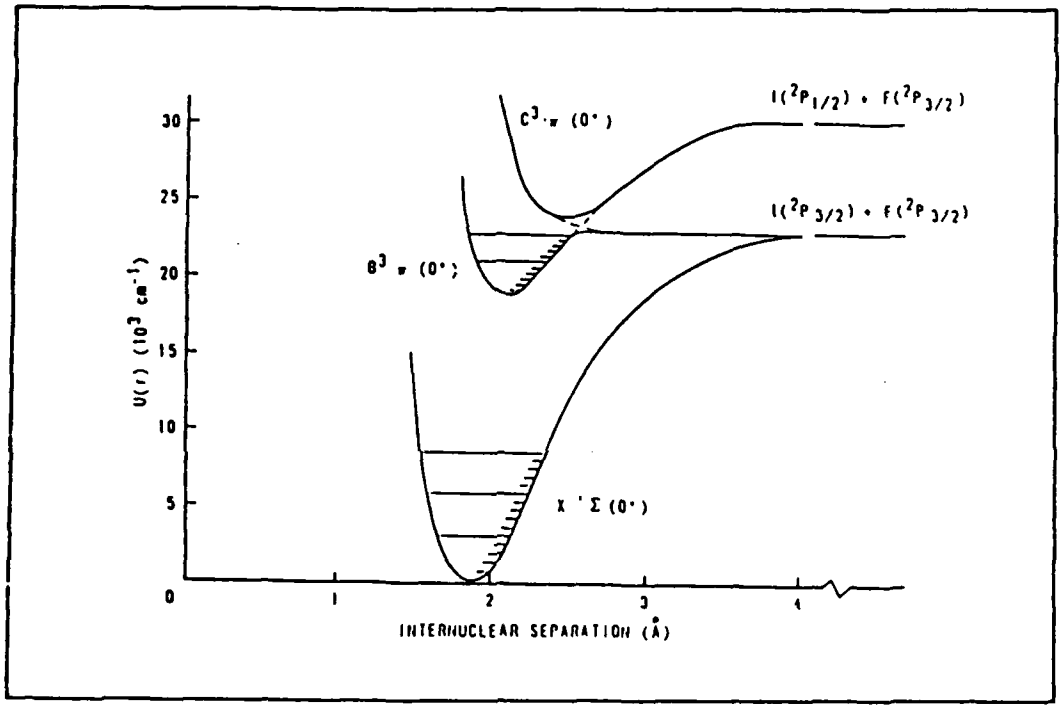

Figure 2.4. Potential Energy Diagram of IF (17:3)

In the two preceding figures, the horizontal axis, r, measures the internuclear distance between the two atoms and has units of angstroms. The vertical axis is energy measured in wave numbers or cm^{-1}. The minima in the curves indicate the equilibrium or lowest energy distance for each state.

Molecular oxygen in the lowest excited electronic state is singlet delta, $O_2(^1\Delta)$. The energy of this excited state is 7918.1 cm^{-1} above the ground state (14:84). It has been shown experimentally that this state has a radiative lifetime of 45 minutes, but when operating in a pressure of 0.5 to 10 torr, the lifetime decreases to about 1 second (12:11). The excited oxygen can be transported for more than a meter without significant losses if 10-20 mm tubing is used (12:11).

Since $O_2(^1\Delta)$ is quenched by metal, a material with a low quenching coefficient should be used to transport the gas. Quartz glass is used to transport the excited oxygen in this experiment.

$O_2(^1\Delta)$ can be produced either chemically or by electric discharge. For this experiment, a microwave electric discharge device operating at 2450 MHz is used. Although both $O_2(^1\Delta)$ and $O_2(^1\Sigma)$ are created by the collisions with the plasma, the lifetime of $O_2(^1\Delta)$ is 10^3 times greater than the $O_2(^1\Sigma)$ lifetime, making the $O_2(^1\Sigma)$ concentration in the gas stream exciting the cavity negligible (15:24).

Kinetic Analysis

There are three proposed mechanisms in the oxygen-IF reaction leading to the excitation of IF from the ground (X) to the B state with subsequent chemiluminescence down to the ground state (6). Each reaction is selected from a set of possible reactions of its type. Figure (2.5) shows an energy level diagram of IF and oxygen. Below are the kinetic reactions for these mechanisms.

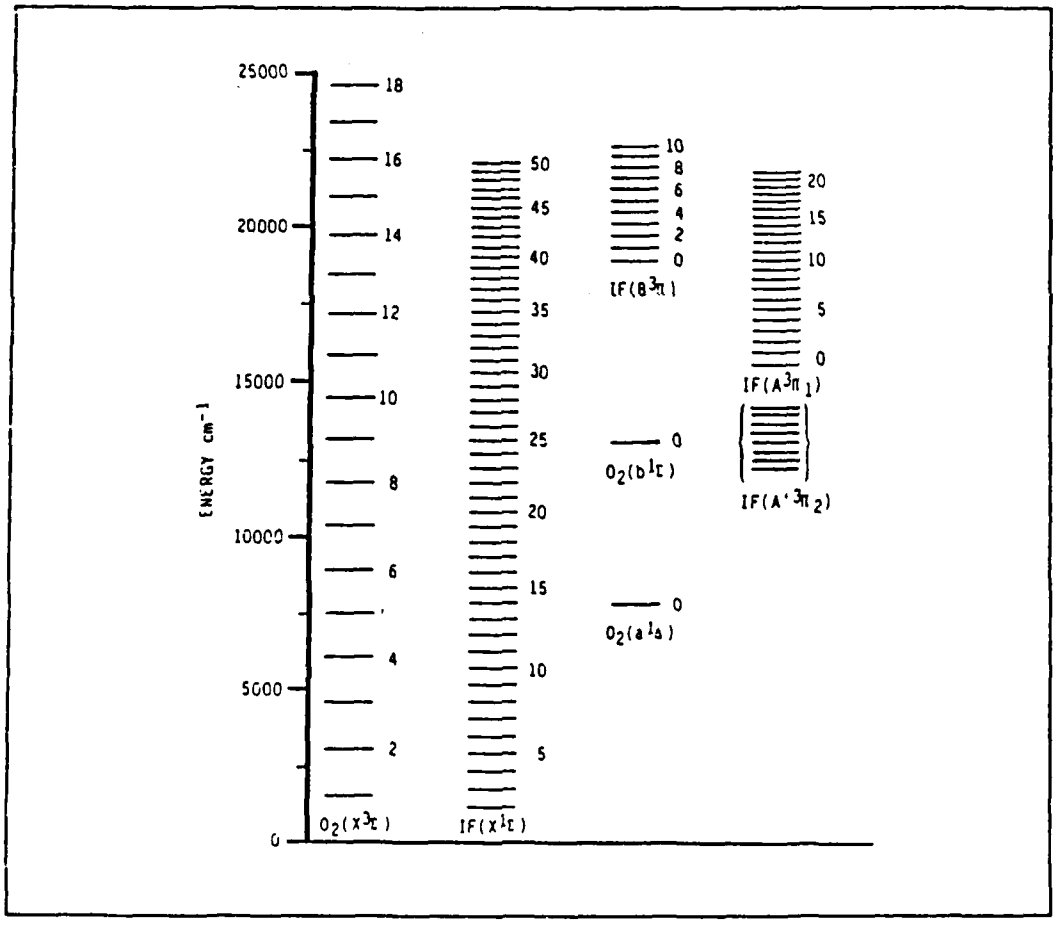

Figure 2.5. Energy Level Diagram of IF and Oxygen (3:3)

Mechanism One.

This mechanism involves an integer number of $O_2(a^1\Delta)$ molecules which provide the IF(X) molecule with the correct amount of energy to excite it to the B state. This postulated reaction mechanism is believed to involve at least three O_2 molecules. From a conservation of energy viewpoint, the $O_2(a^1\Delta)$ molecule in the zero vibrational state has about 7918 cm^{-1} of energy. Three times this energy gives at least the 19054 cm^{-1} of energy required to reach the IF(B) state.

The reaction begins with the interaction of a ground state IF molecule and an integer number (n) of $O_2(a^1\Delta)$ molecules, and proceeds at rate k_1.

$$IF(X^1\Sigma) + n\ O_2(a^1\Delta) \xrightarrow{k_1} IF(B^3\Pi) + n\ O_2(X^3\Sigma) \qquad (2.8)$$

The excited IF(B) molecule then relaxes down to its ground state and a photon is released. This reaction takes place at the rate of $1/\tau$.

$$IF(B^3\Pi) \xrightarrow{1/\tau} IF(X^1\Sigma) + h\nu \qquad (2.9)$$

The rate at which the concentration of IF(B) changes with time is given by

$$\frac{d[IF(B^3\Pi)]}{dt} = k_1[IF(X^1\Sigma)][O_2(a^1\Delta)]^n - \frac{1}{\tau}[IF(B^3\Pi)] \qquad (2.10)$$

The steady state concentration of IF(B) is

$$[IF(B^3\Pi)] = \tau\, k_1\, [IF(X^1\Sigma)][O_2(a^1\Delta)]^n \qquad (2.11)$$

But the intensity of the chemiluminescence (I) from the IF(B) molecules is proportional to the IF(B) concentration.

$$I \propto [IF(B^3\Pi)] \qquad (2.12)$$

So, the intensity can be written as

$$I \propto \tau\, k_1\, [IF(X^1\Sigma)][O_2(a^1\Delta)]^n \qquad (2.13)$$

The natural log is taken of both sides of eq (2.13), yielding

$$\ln(I) \propto n \ln [O_2(a^1\Delta)] + \text{constant} \qquad (2.14)$$

A plot of eq (2.14) produces a straight line with a slope n, where n equals the number of $O_2(a^1\Delta)$ molecules that raise the IF molecule from the ground to the excited state. As

mentioned, because of energy considerations, n will be at least three.

Figure (2.6) is an energy diagram which shows the reactions for mechanism one.

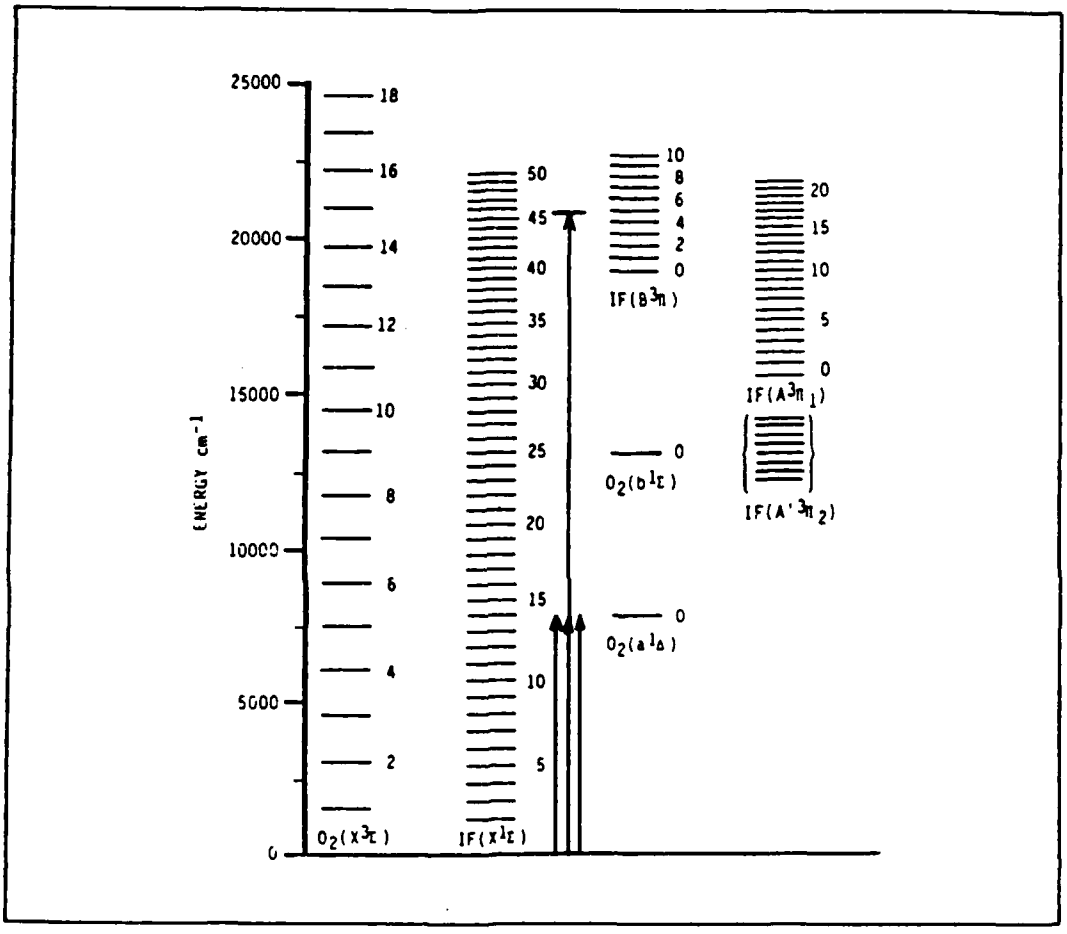

Figure 2.6. Energy Level Diagram of Mechanism One Reactions

Mechanism Two.

This mechanism is a 2-step mechanism in which two $O_2(a^1\Delta)$ molecules raise $IF(X^1\Sigma)$ to the $IF(A'^3\Pi_2)$ state. Then, a third $O_2(a^1\Delta)$ molecule reacts with the IF in the A' state to yield $IF(B^3\Pi)$. The governing reactions are as follows:

$$2\ O_2(a^1\Delta) \xrightarrow{k1} O_2(b^1\Sigma) + O_2(X^3\Sigma) \qquad (2.15)$$

$$O_2(b^1\Sigma) + IF(X^1\Sigma) \xrightarrow{k2} IF^{\dagger}(A'^3\Pi_2) + O_2(X^3\Sigma) \qquad (2.16)$$

$$IF^{\dagger}(A'^3\Pi_2) + O_2(a^1\Delta) \xrightarrow{k3} IF(B^3\Pi) + O_2(X^3\Sigma) \qquad (2.17)$$

The IF in the excited B state then emits a photon:

$$IF(B^3\Pi) \xrightarrow{1/\tau} IF(X^1\Sigma) + h\nu \qquad (2.18)$$

The time rate of change of the IF(B) concentration is given by

$$\frac{d[IF(B^3\Pi)]}{dt} = k3\ [O_2(a^1\Delta)][IF^{\dagger}(A'^3\Pi_2)] - \frac{1}{\tau}[IF(B^3\Pi)] \qquad (2.19)$$

Under steady state conditions, from eq (2.19), the chemiluminescent intensity is proportional to the concentration of $O_2(a^1\Delta)$ and $IF^\dagger(A'^3\Pi_2)$:

$$I \propto \tau\, k_3 \left[O_2(a^1\Delta)\right]\left[IF^\dagger(A'^3\Pi_2)\right] \qquad (2.20)$$

But, the desired intensity measurement should only be a function of the O_2 concentration. So, from eqs (2.16), and (2.17), the following rate equation can be written

$$\frac{d\left[IF(A'^3\Pi_2)\right]}{dt} = k_2 \left[O_2(b^1\Sigma)\right]\left[IF(X^1\Sigma)\right] - k_3\left[IF^\dagger(A'^3\Pi_2)\right]\left[O_2(a^1\Delta)\right] \qquad (2.21)$$

Solving this equation for the concentration of $IF^\dagger(A'^3\Pi_2)$

$$\left[IF^\dagger(A'^3\Pi_2)\right] = \frac{k_2}{k_3}\,\frac{\left[O_2(b^1\Sigma)\right]\left[IF(X^1\Sigma)\right]}{\left[O_2(a^1\Delta)\right]} \qquad (2.22)$$

But, by combining eqs (2.15) and (2.22) from above, the following equation can be written for the time rate of change of $\left[O_2(b^1\Sigma)\right]$:

$$\frac{d\left[O_2(b^1\Sigma)\right]}{dt} = k_1\left[O_2(a^1\Delta)\right]^2 - k_2\left[O_2(b^1\Sigma)\right]\left[IF(X^1\Sigma)\right] \qquad (2.23)$$

Under steady state conditions, the concentration of $O_2(b^1\Sigma)$ can be solved as

$$[O_2(b^1\Sigma)] = \frac{k1}{k2} \frac{[O_2(a^1\Delta)]^2}{[IF(X^1\Sigma)]} \quad (2.24)$$

Substituting eq (2.24) into eq (2.22) and solving for the $IF^+(A'^3\Pi_2)$ concentration yields

$$[IF^+(A'^3\Pi_2)] = \frac{k2}{k3} \frac{k1}{k2} \frac{[O_2(a^1\Delta)]^2 [IF(X^1\Sigma)]}{[IF(X^1\Sigma)] [O_2(a^1\Delta)]} \quad (2.25)$$

which can be simplified to yield

$$[IF^+(A'^3\Pi_2)] = \frac{k1}{k3} [O_2(a^1\Delta)] \quad (2.26)$$

The intensity of the chemiluminescence is proportional to the concentration of $O_2(a^1\Delta)$ as

$$I \propto \tau\, k3[O_2(a^1\Delta)] \frac{k1}{k3}[O_2(a^1\Delta)] \quad (2.27)$$

Eq (2.27) can be simplified to yield an expression for the intensity that is not a function of the IF(B) concentration:

$$I \propto \tau\, k1[O_2(a^1\Delta)]^2 \quad (2.28)$$

Taking the natural log of both sides of eq (2.28) gives

$$\ln(I) \propto 2 \ln [O_2(a^1\Delta)] + \text{constant} \qquad (2.29)$$

A plot of eq (2.29) produces a straight line with a slope of two.

Figure (2.7) is an energy diagram which shows the reactions for mechanism two.

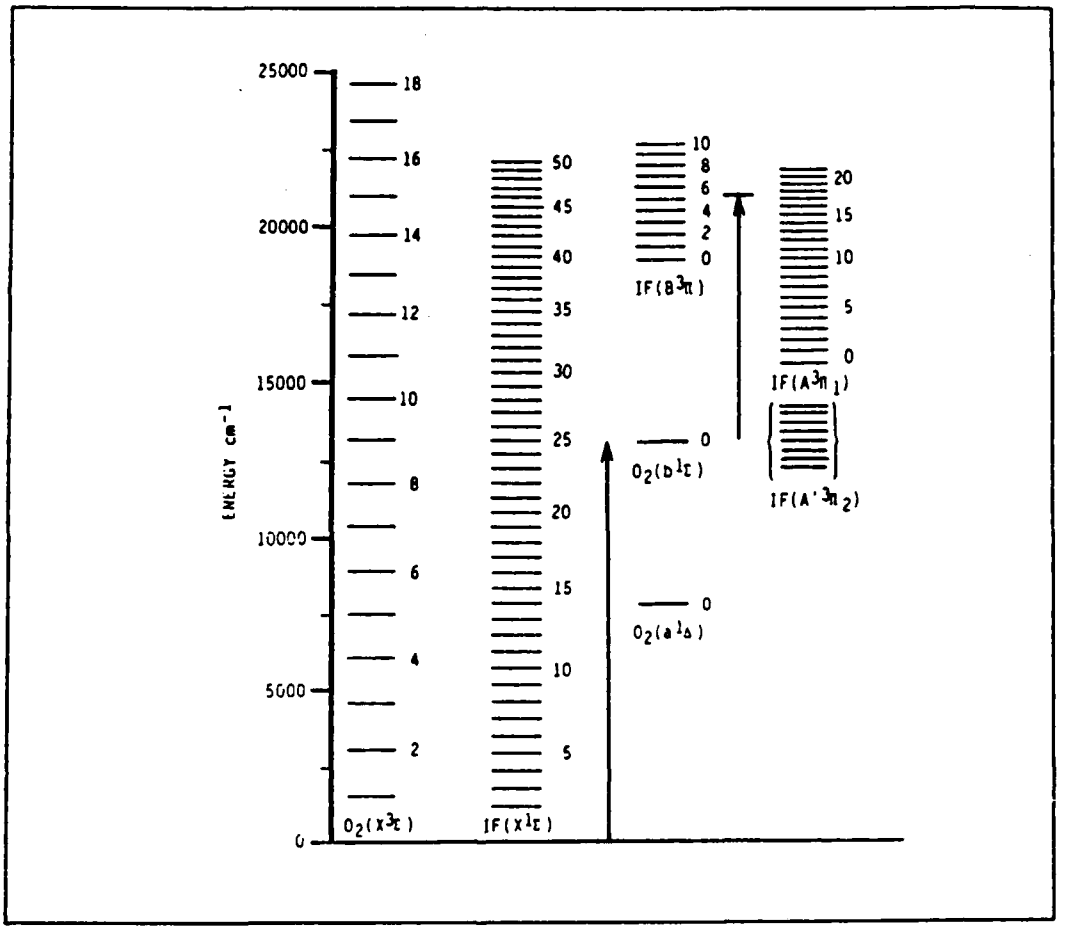

Figure 2.7. Energy Level Diagram of Mechanism Two Reactions

Mechanism Three.

This mechanism involves the reaction of three $O_2(a^1\Delta)$ molecules that raise the IF molecule from the ground to the excited state. Each O_2 molecule in the "a" state raises the IF molecule to a higher vibrational and rotational level within the ground electronic state. Three O_2 molecules provide the IF(X) molecule with the correct amount of energy to align it with the IF(B) state. The reactions that govern this energy exchange are as follows:

$$IF(X^1\Sigma) + O_2(a^1\Delta) \xrightarrow{k1} IF(X,v'') + O_2(X^3\Sigma) \qquad (2.30)$$

$$IF(X,v'') + O_2(a^1\Delta) \xrightarrow{k2} IF(X,v''') + O_2(X^3\Sigma) \qquad (2.31)$$

$$IF(X,v''') + O_2(a^1\Delta) \xrightarrow{k3} IF(B^3\Pi) + O_2(X^3\Sigma) \qquad (2.32)$$

The excited IF(B) molecule then relaxes down to its ground state and a photon is released. This reaction is shown below in eq (2.33):

$$IF(B^3\Pi) \xrightarrow{1/\tau} IF(X^1\Sigma) + h\nu \qquad (2.33)$$

The time rate of change of IF(B) is given by the following equation:

$$\frac{d[IF(B^3\Pi)]}{dt} = k_3 [IF(X,v''')][O_2(a^1\Delta)] - \frac{1}{\tau} [IF(B^3\Pi)] \qquad (2.34)$$

In the steady state, eq (2.34) equals zero, and the concentration of IF(B) can be solved to yield

$$[IF(B^3\Pi)] = \tau k_3 [IF(X,v''')][O_2(a^1\Delta)] \qquad (2.35)$$

The chemiluminescent intensity is again proportional to the IF(B) concentration, as

$$I \propto \tau k_3 [IF(X,v''')][O_2(a^1\Delta)] \qquad (2.36)$$

But the intensity should only be a function of the O_2 concentration, so from the kinetic equations containing IF(X,v''') and IF(X,v''), the following two equations can be written as:

$$[IF(X,v''')] = \frac{k_2}{k_3} \frac{[IF(X,v'')][O_2(a^1\Delta)]}{[O_2(a^1\Delta)]}$$

$$= \frac{k_2}{k_3} [IF(X,v'')] \qquad (2.37)$$

$$[IF(X,v'')] = \frac{k_1}{k_2} \frac{[IF(X^1\Sigma)][O_2(a^1\Delta)]}{[O_2(a^1\Delta)]}$$

$$= \frac{k_1}{k_2} [IF(X^1\Sigma)] \qquad (2.38)$$

Combining eqs (2.37) and (2.38) gives an expression for the IF(X,v''') concentration:

$$[IF(X,v''')] = \frac{k_1}{k_3} [IF(X^1\Sigma)] \qquad (2.39)$$

Eq (2.39) can be combined with eq (2.35) to yield the chemiluminescent intensity:

$$I \propto \tau k_3 \frac{k_1}{k_3} [IF(X^1\Sigma)][O_2(a^1\Delta)]$$

$$= \tau k_1 [IF(X^1\Sigma)][O_2(a^1\Delta)] \qquad (2.40)$$

Taking the natural log of both sides of eq (2.40) gives

$$\ln(I) \propto \ln [O_2(a^1\Delta)] + \text{constant} \qquad (2.41)$$

A plot of eq (2.41) produces a straight line with a slope of one.

Figure (2.8) is an energy diagram which shows the reactions for mechanism three.

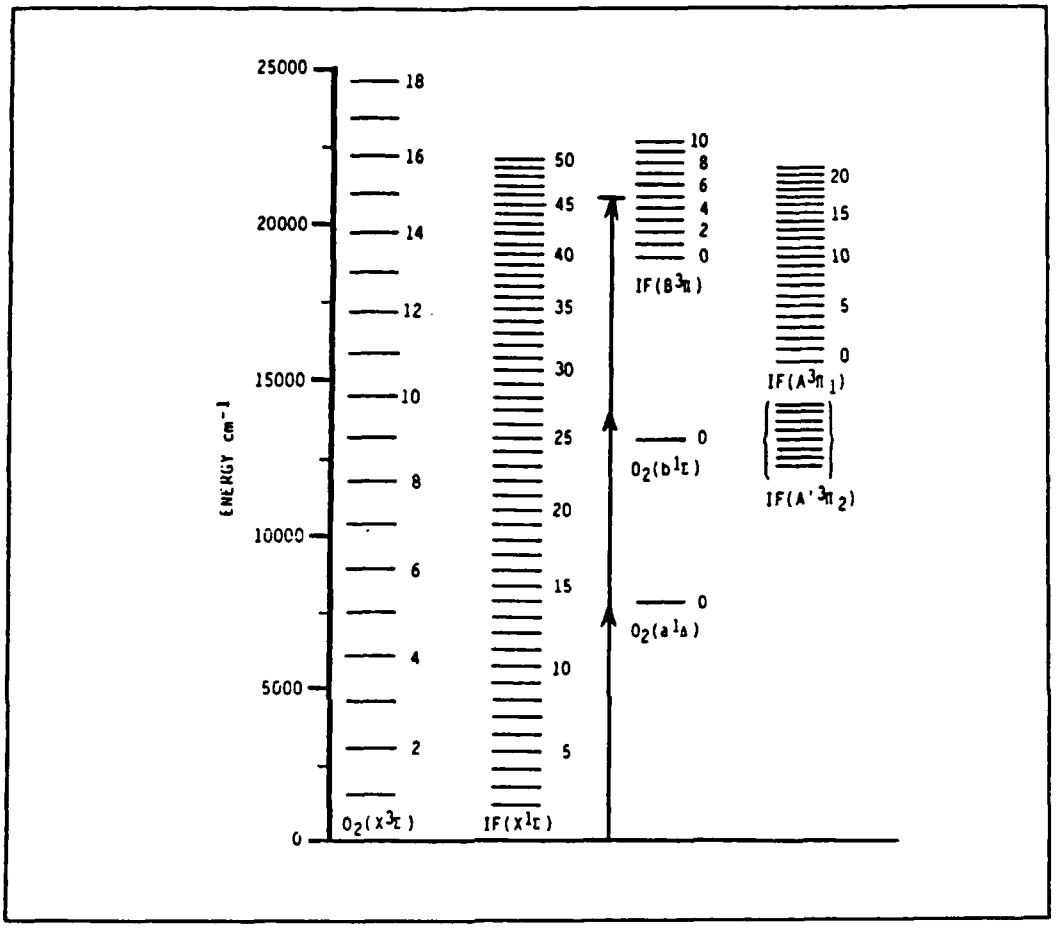

Figure 2.8. Energy Level Diagram of Mechanism Three Reactions

Depending on the responsible mechanism, the chemiluminescence associated with the IF(B⟶X) transition should be proportional to the first, second, or third power of the $O_2(^1\Delta)$ concentration.

III. Experimental Apparatus

Introduction

This section describes the experimental apparatus used in this experiment. First, a general description of the flow tube reactor is given, and then an analysis of its major components is presented. Finally, a description of the detection and measurement system is provided.

Flow Tube System

The flow tube reactor system used for this experiment is shown as a block diagram in Figure (3.1). The system consists of three main component systems:

(1) Vacuum

(2) Flow Tube

(3) Optical train.

Each component system is discussed below.

Vacuum. The vacuum system is driven by a Sergeant-Welch, Model 1375 vacuum pump. A ball valve at the input of the pump allows the flow tube system to be isolated from the pump. This valve can also be used to vary the flow rate of the pump. A 1 inch outside diameter (OD) stainless steel tube connects the valve and pump to the cold trap. The cold trap connects to the 1 inch stainless steel tube through a 1/2 inch Cajon connector welded to the tube.

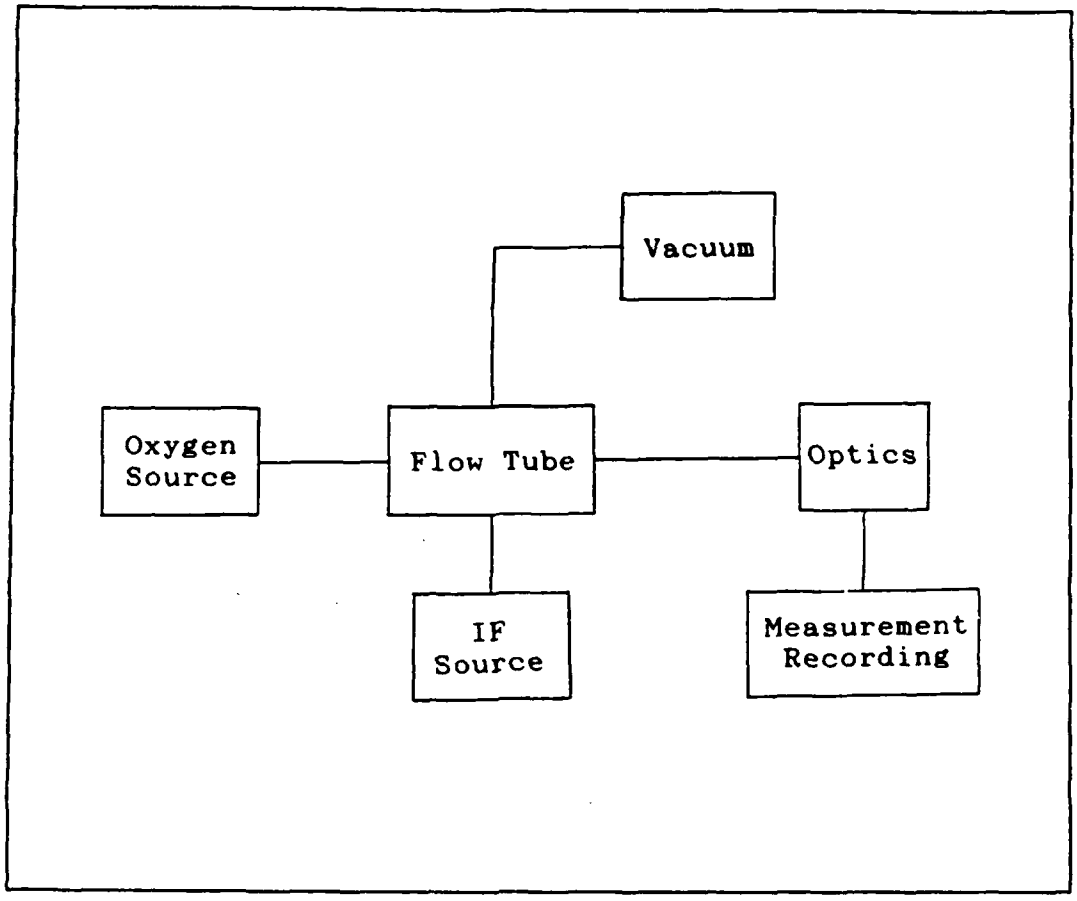

Figure 3.1. Flow Tube Reactor Block Diagram

The cold trap is fabricated from 1/2 inch OD copper tubing. The trap is thermally isolated from the system by 1/2 inch inside diameter (ID) teflon connectors. These connectors, made by Fluorocarbon Handling Devices, are used throughout the vacuum and flow tube systems to connect all 1/2 inch OD pieces. A 1/2 inch stainless steel pipe connects the cold trap to the top of the 6-way cross.

Flow Tube. The 6-way cross is the main part of the flow tube, and it is where the chemiluminescent flame exists. Figure (3.2) is a schematic diagram of the six-way cross and the input to each of the ports.

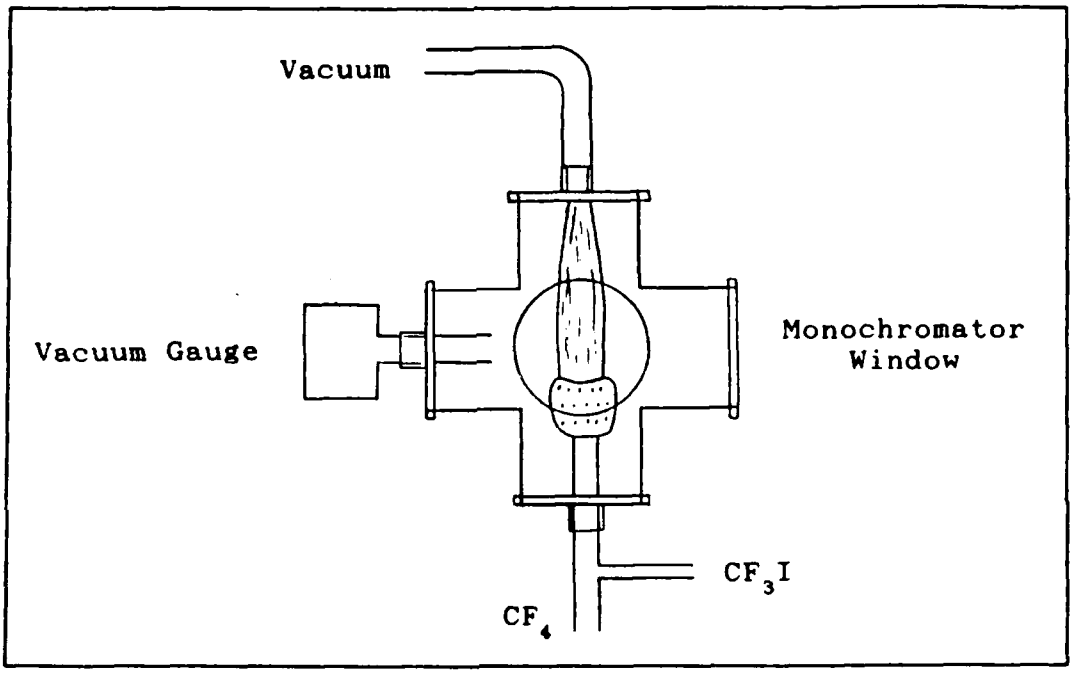

Figure 3.2. Schematic of Six-way Cross and Inputs

Two of the ports are covered with plexiglas windows. One of the windows faces the monochromator and the other window is used as a viewing port. The remaining four ports have 1/2 inch Cajon feed-through connectors welded to

stainless steel plates. The four Cajon connectors have the following inputs:

(1) Vacuum System

(2) Baratron Pressure Gauge

(3) Oxygen Inlet Tube

(4) IF Inlet Tube.

The oxygen and IF generation and inlets are described below.

The oxygen inlet tube was described by Ritchey and is not changed for this experiment (12:26-27). $O_2(^1\Delta)$ is generated using a 2450 MHz microwave discharge by the same procedures outlined by Ritchey except that aluminum oxide tubes are used in the microwave cavities instead of quartz glass (12:28).

Figure (3.3) shows the valve and bypass system used to control the flow of molecular oxygen through the microwave cavity, and thereby control the concentration of $O_2(^1\Delta)$. By maintaining the total oxygen flow constant and monitoring the bypassed flow, the amount of oxygen passing through the microwave cavity is known, and the relative $O_2(^1\Delta)$ concentration can be determined.

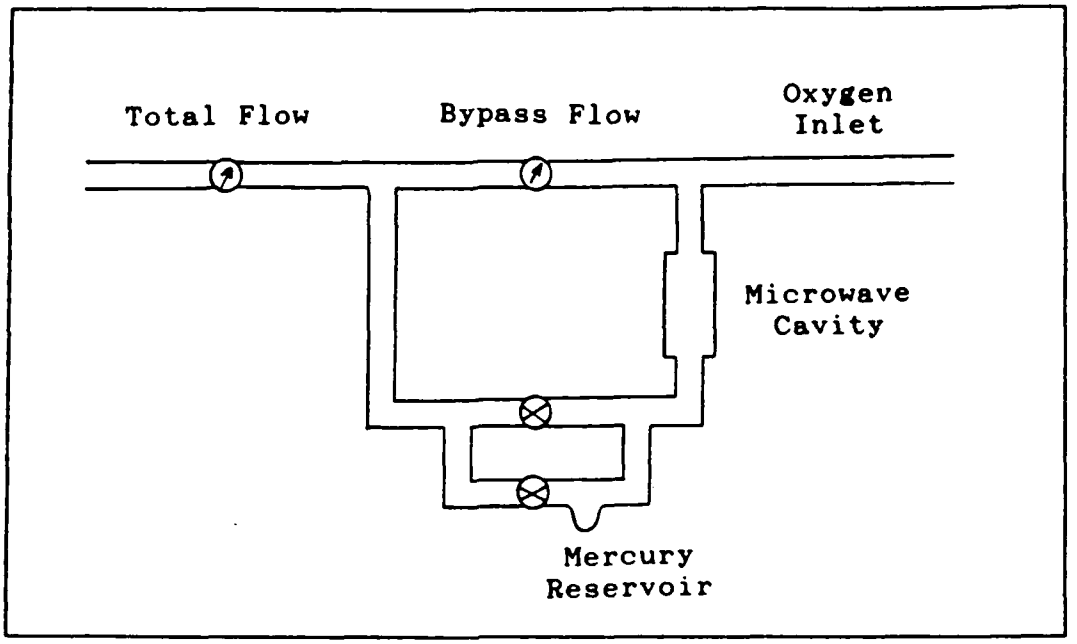

Figure 3.3. Oxygen Valve and Bypass System

A dual valve system is used prior to the oxygen microwave discharge cavity to allow the oxygen inlet tube to be coated with mercuric oxide, HgO. When the branch containing the mercury is open, mercury vapor flows through the microwave cavity and mercuric oxide is formed. This coating quenches any atomic oxygen that may exist at the oxygen inlet (7:11).

Figure (3.4) depicts the IF and oxygen inlet tubes. The IF inlet consists of a 1/4 inch quartz CF_3I inlet tube connected to a 1/2 inch quartz CF_4 inlet tube. IF(X) is produced in this tube and is brought into the base of the oxygen inlet tube.

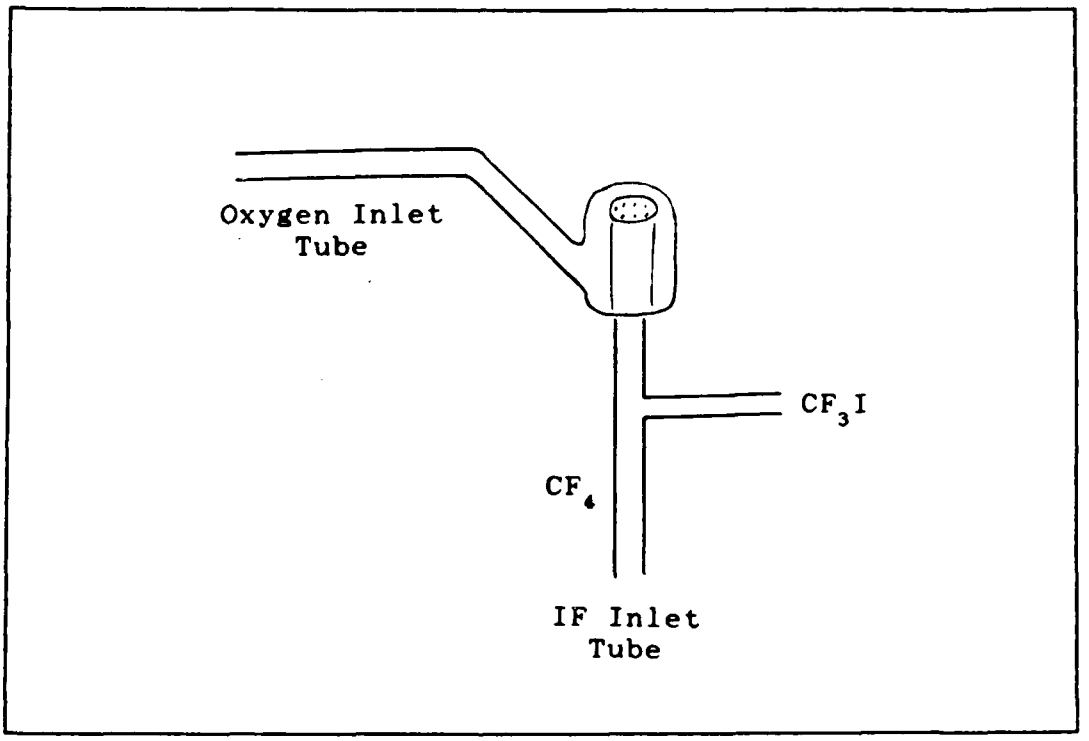

Figure 3.4. IF and Oxygen Inlet Tubes

The IF inlet tube is coated with halocarbon wax to prevent dissociation of the IF molecules due to wall collisions (6). The reactions governing the creation of ground state IF are given below.

Initially CF_4 is passed through a 2450 MHz microwave discharge cavity creating CF_3 radicals and fluorine atoms. The fluorine atoms react with the CF_3I molecules to form IF(X) and CF_3 (13:1128). Wall effects break the CF_3 down to C_2F_6 and can cause the IF(X) to break down to IF_3 and IF_5 (6). The halocarbon wax helps prevent this second reaction. The ground state IF then enters the bottom of the oxygen inlet tube where it reacts with the $O_2(^1\Delta)$ to form IF(B).

Throughout the system, 1/4 inch copper tubing is used to bring the gas supplies to their respective inputs.

Optics Train. The chemiluminescent flame is focused on the monochromator slit by a 15 cm focal length, glass collecting lens. The lens diameter and focal length are chosen so as to allow for good resolution in the 0.3 meter McPherson scanning monochromator, which was located 60 cm from the flame.

Detection and Measurement

The detector is an RCA C31034-02 photomultiplier tube (PMT). The PMT is attached to the monochromator with a thermoelectric refrigerated chamber as described by Ritchey (12:29). The PMT utilizes a gallium arsenide photocathode, and has a spectral response from 2500 to 8500 Å (11:3).

The PMT connects to an EG&G Princeton Applied Research Model 1121A Discriminator Control Unit which provides the bias voltage for the PMT. An EG&G Model 1112 Photon Counter/Processor provides a digital readout of the photon

count. An X-Y plotter is used to record the spectrum during a monochromator scan.

In order to observe the broadband spectrum of the flame, the monochromator grating is adjusted to the zeroth order. This setting scatters a portion of the input off of the grating and onto the output slit. The PMT then accepts the output from the monochromator and the photon counting system indicates the number of photons received over a unit time. The $O_2(^1\Delta)$ concentration is then varied and the flame intensity is registered.

IV. Experimental Procedures

Introduction

This section details the experimental operation and data collection performed in this thesis. A procedural description is given following the course of the experiment. System alignment and calibration is also discussed. Problems or notes of interest are addressed in the relevant sections.

General Procedures

After pumping the system to near zero torr, the rate of CF_4 flow is increased until the total pressure reaches 0.34 torr. The oxygen flow rate is then increased until the total pressure reaches 2.14 torr or increases by 1.80 torr. In order to make small adjustments in pressure, a digital volt meter is attached to the analog Baratron pressure gauge.

The flow-control valve at the input of the vacuum pump is adjusted for the minimum flow rate that will still maintain a vacuum. If the valve is not properly adjusted, the component gases are used at an excessive rate.

Next, the microwave discharge cavities on the CF_4 and O_2 inputs are struck using a tesla coil. Stabilizing the plasma is difficult even though the cooling procedures outlined by Duray are followed (7:32-34).

It is very important to tune the cavities for minimum reflected power. When the cavities are properly tuned, it

is possible to achieve near zero reflected power for 80 watts forward power. If the cavities are not properly adjusted, they operate at higher temperatures and can arc causing damage to the aluminum oxide tubes. It is possible to get a leak in the tube if the arcing is not stopped by immediately turning off the power supply. The plasma should then be re-ignited with the tesla coil. Over-heated aluminum oxide tubes can also melt the teflon connectors and cause a vacuum leak.

The CF_3I is next added to increase the pressure by 0.02 to 0.03 torr yielding a total pressure of about 2.16 torr. The flow rate of CF_3I is very small compared to the other constituent gases, and must be adjusted slowly to yield the maximum flame intensity. Other gas flow-rate combinations do result in a chemiluminescent flame, but these values are considered to be optimal for gas conservation and flame intensity. Slight flow-rate variations may be necessary to achieve optimal flame intensity.

Because the CF_3I is a liquid at room temperature, a room-temperature water bath may be needed to increase the gas vapor pressure enough to pump the CF_3I from the cylinder.

The oxygen inlet tube is coated with HgO by the same procedure outlined by Duray to insure that atomic oxygen is removed (7:33).

While keeping the total oxygen flow rate constant, some oxygen is allowed to flow through the oxygen bypass. This

procedure allows the bypassed oxygen to flow directly into the oxygen inlet and not pass through the microwave cavity. In this way, the concentration of $O_2(^1\Delta)$ is varied without changing the total oxygen concentration. Flame intensity readings are recorded for various excited oxygen concentrations.

Since the total flow of oxygen must be kept constant, and because the vacuum pump is connected to the flow tube by stainless steel and copper pipes, some table vibration occurs. This pump vibration can cause vibrations in the flow meters, which makes precise readings difficult. This vibration adds to the experimental error in the analysis.

Because toxic gases are created by this experiment, the pump exhaust is vented to the hood.

Alignment and Calibration

Alignment of the optical train is accomplished using a mercury pen light placed in the six-way cross at the flame origin to approximate the flame position. The flame occurs directly above the oxygen inlet tube opening, because the lifetime of IF(B) is between 0.44 and 8.8 μs (2:172). The monochromator and collecting lens are positioned for the maximum intensity at the input and output slit of the monochromator. Fine alignment is accomplished by adjusting the monochromator and collecting lens for maximum photon count at one of the mercury lines.

Oriel pen lamps are used for spectra calibration. Mercury and xenon lamps are used because they have peaks in the 5700 to 6200 Å band.

Because of the flame's low light level, the signal-to-noise (S/N) ratio of the PMT is a concern. The high voltage and discriminator threshold settings are adjusted to yield the highest S/N ratio. The PMT is operated at -25°C, and after setting the high voltage and discriminator threshold levels, the PMT dark count is approximately 22 per second with the room lights off. The optimum high voltage value is 1300 volts. Typical peak counts during a spectral scan are 325 per second.

The monochromator slit widths are varied between 50 and 250 μm in an effort to maximize the resolution and signal. The final setting depends on the flame intensity, which varies with gas combinations and pressures.

A resistor-capacitor (RC) low pass filter is used to filter out high-frequency noise contained in the amplifier/discriminator output. The RC filter shunts the noise to ground, but allows the plotter to respond to the average signal intensity, important at low signal levels. By using this procedure, a spectral plot of IF(B$\rightarrow$X) is obtained.

V. Results

Introduction

This section contains the observations and analysis of the data that were collected during the experiments. First, the experimental observations are discussed, with emphasis on critical procedures and experimental error. Then, the data are analyzed and the results are compared to the proposed reaction mechanism models.

Flow Tube Observations

The chemiluminescent flame from the IF(B⟶X) transition was initially difficult to obtain. Problems were traced to improper microwave cavity tuning and plasma instability.

The reflected power meter on the microwave power supply is used to tune the cavity for minimum reflected power. A reflected power between zero and two watts is ideal. Unless the cavity is cooled, however, the plasma state changes which causes a change in impedance. This impedance change brings about a change in the flame intensity. Only after the cavities are cooled by the procedure described by Duray does the flame intensity stabilize (7:32-34).

After the flame was made stable, there were difficulties recording the spectrum on the X-Y plotter. With signal-to-noise power ratios between 3 and 16, the peak intensities were often hidden in the noise. In order to improve the spectral plot, a low-pass filter was added to the plotter input.

The Davis team produced a spectral scan showing the chemiluminescence from the IF(B⟶X) transitions (3:16). This scan is shown in Figure (5.1).

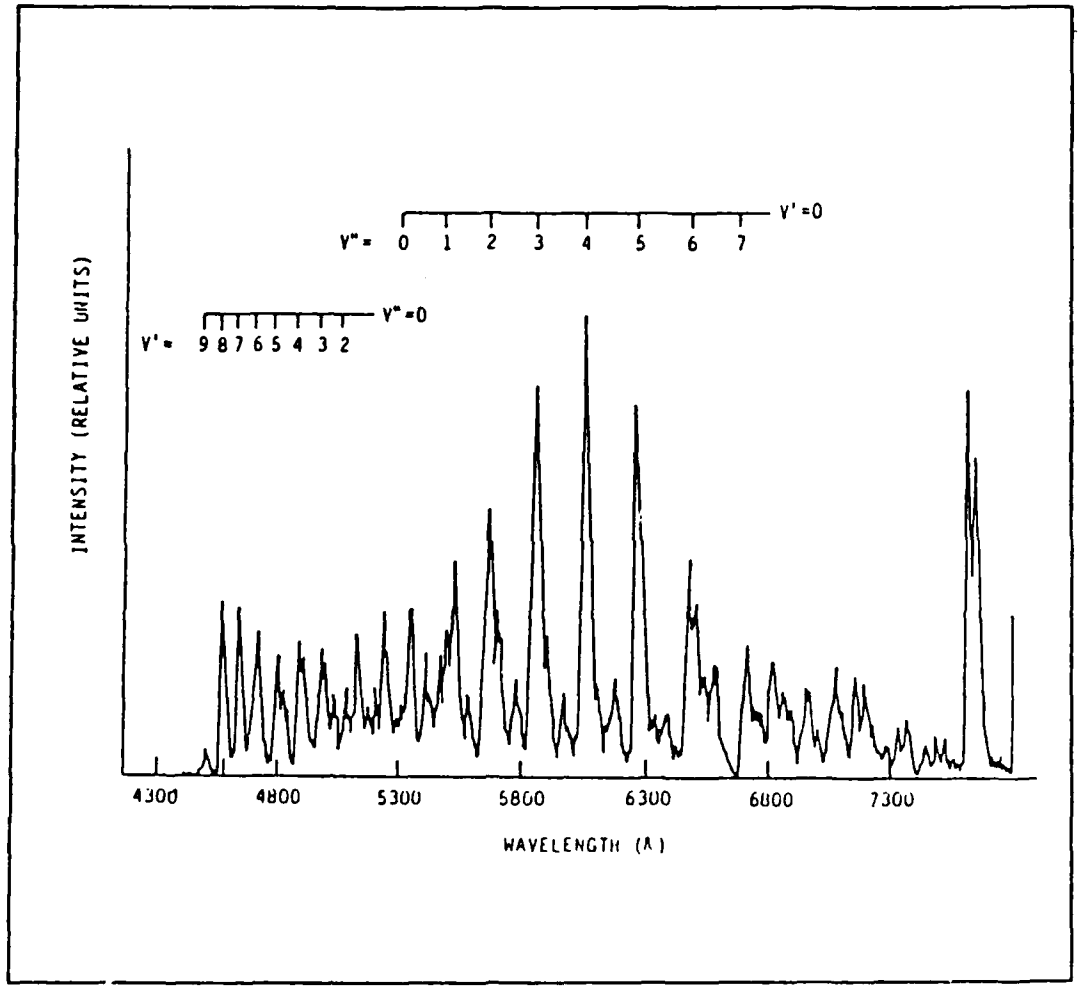

Figure 5.1. Spectral Scan of Chemiluminescence from IF(B⟶X) (3:16)

Figure (5.2) shows the spectrum recorded on the X-Y plotter. Several monochromator slit widths were tested, but due to the low flame intensities, the best spectrum was obtained when input and output slits were both set to 200 μm. The monochromator grating had 1200 lines per mm blazed at 7500 Å.

A comparison of Figures (5.1) and (5.2) clearly shows the dominant 3-0, 4-0, and 5-0 transitions. The intensity amplitudes in Figure (5.2) appear low because the spectrum was photographically reduced.

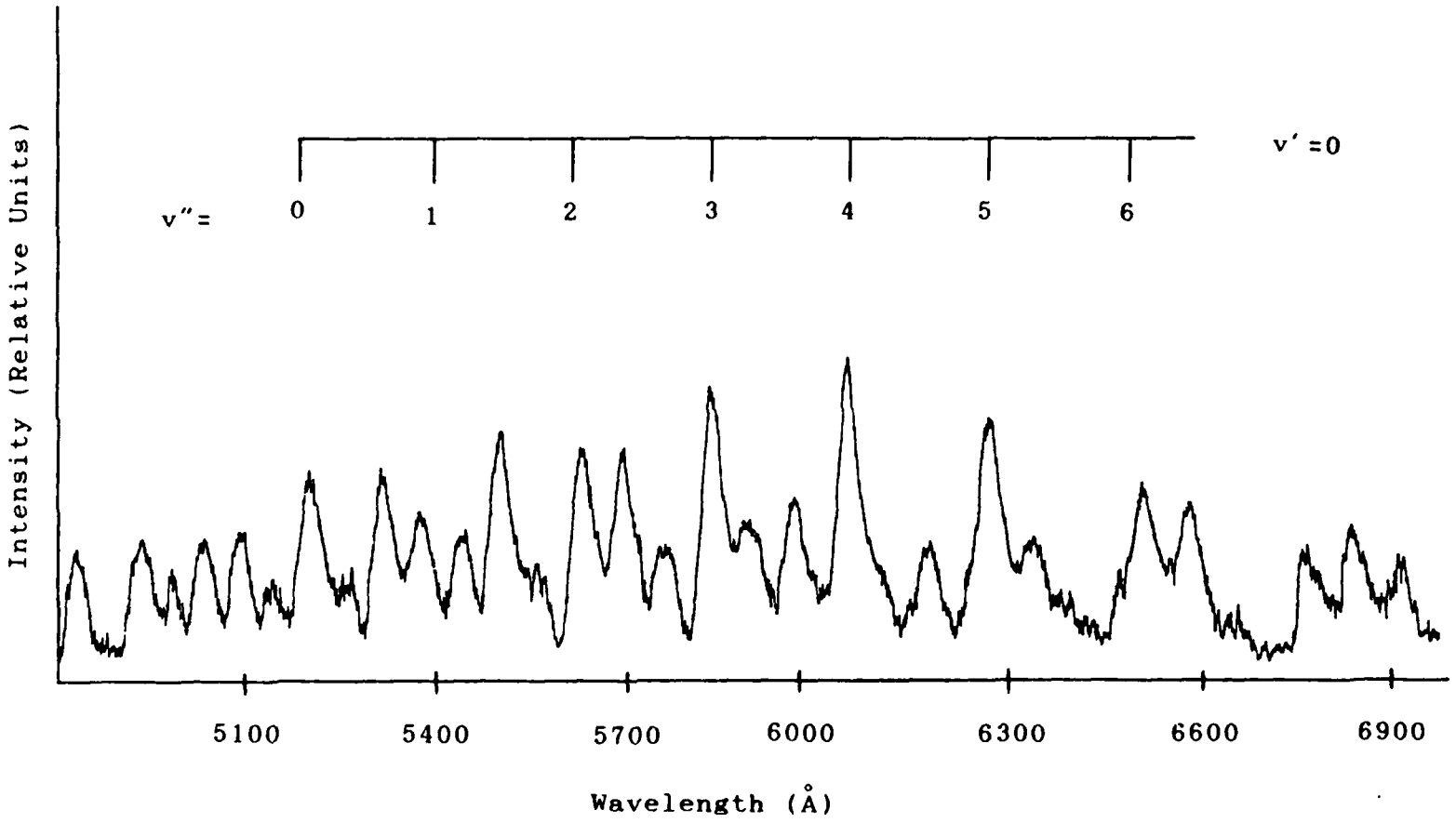

Figure 5.2. Experimental Spectral Scan of IF(B⟶X) Chemiluminescence

Kinetics

Data was taken for various pressure and flow rate combinations from a total pressure of 1.50 to 4.10 torr. A total pressure of 2.16 torr was found to produce a bright flame while not using the component gases too rapidly. Tables (5.1) and (5.2) list the data collected for two representative samples.

TABLE 5.1

Flame Intensity as a Function of Percent Flow:

Data Set One

Count	ln (Count)	% Flow*	ln (% Flow)
6.63 E3	8.80	100.00	4.61
6.42 E3	8.77	94.19	4.55
6.16 E3	8.73	91.86	4.52
5.83 E3	8.67	88.37	4.48
3.30 E3	8.10	59.30	4.08
1.87 E3	7.53	30.23	3.41
1.24 E3	7.12	18.60	2.92
9.30 E2	6.84	6.98	1.94

* Corresponds to the relative $O_2(^1\Delta)$ concentration.

TABLE 5.2

Flame Intensity as a Function of Percent Flow:

Data Set Two

Count	ln (count)	% Flow*	ln (% Flow)
7.90 E3	8.97	100.00	4.61
7.70 E3	8.95	94.19	4.55
7.60 E3	8.94	88.37	4.48
6.90 E3	8.84	76.74	4.34
6.87 E3	8.83	65.12	4.18
6.36 E3	8.76	53.49	3.98
4.10 E3	8.32	41.86	3.73
2.90 E3	7.97	30.23	3.41
1.27 E3	7.15	18.60	2.92
8.60 E2	6.76	6.98	1.94

* Corresponds to the relative $O_2(^1\Delta)$ concentration.

In the two previous data sets, the partial pressures of $O_2/CF_4/CF_3I$ were 1.80/0.34/0.02 torr, yielding a total pressure of 2.16 torr.

The data are graphed in Figures (5.3) and (5.4). Linear regression analysis was performed on the data points to fit a line to the data.

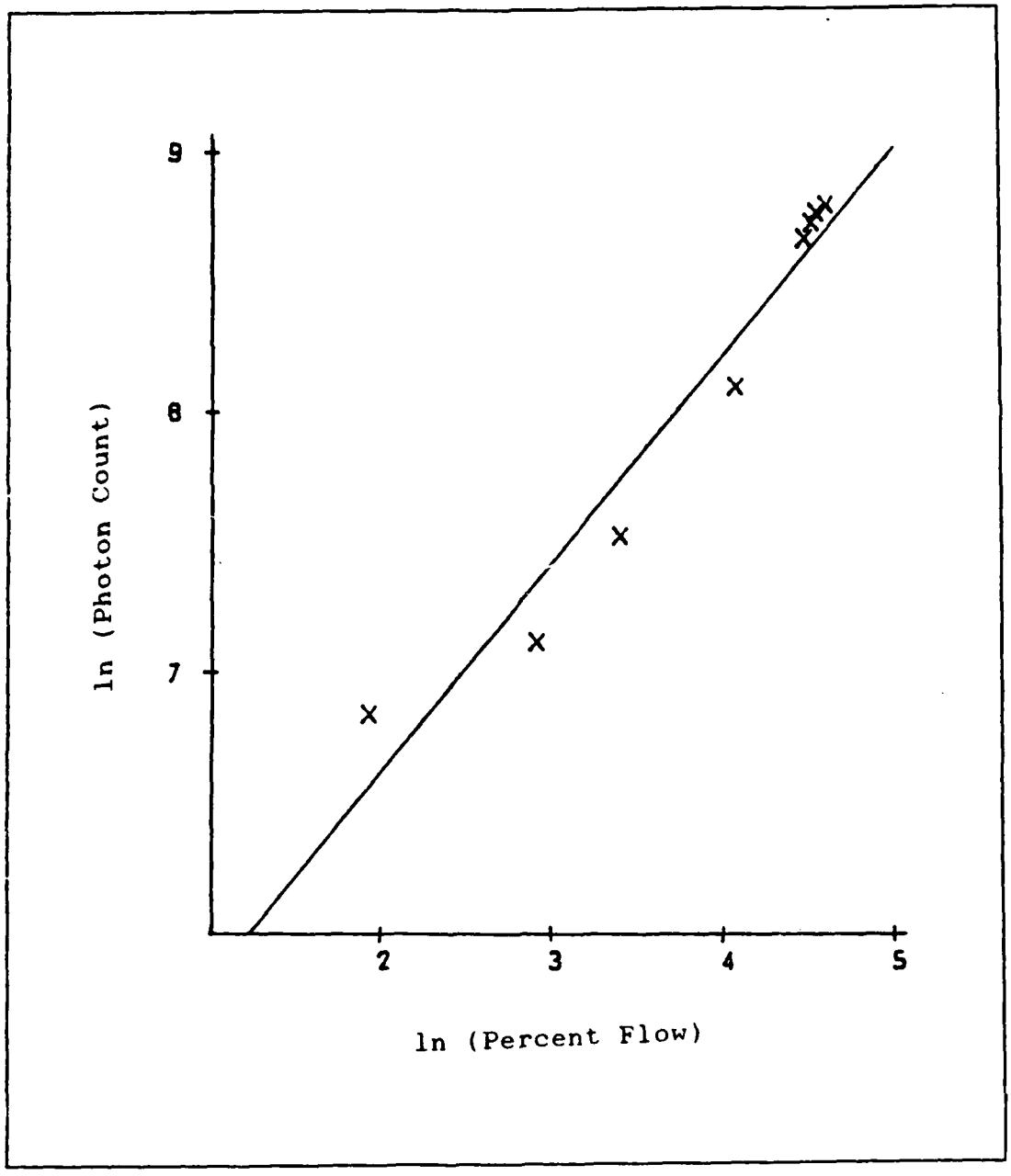

Figure 5.3. Graph of Flame Intensity as a Function of Percent Flow: Data Set One

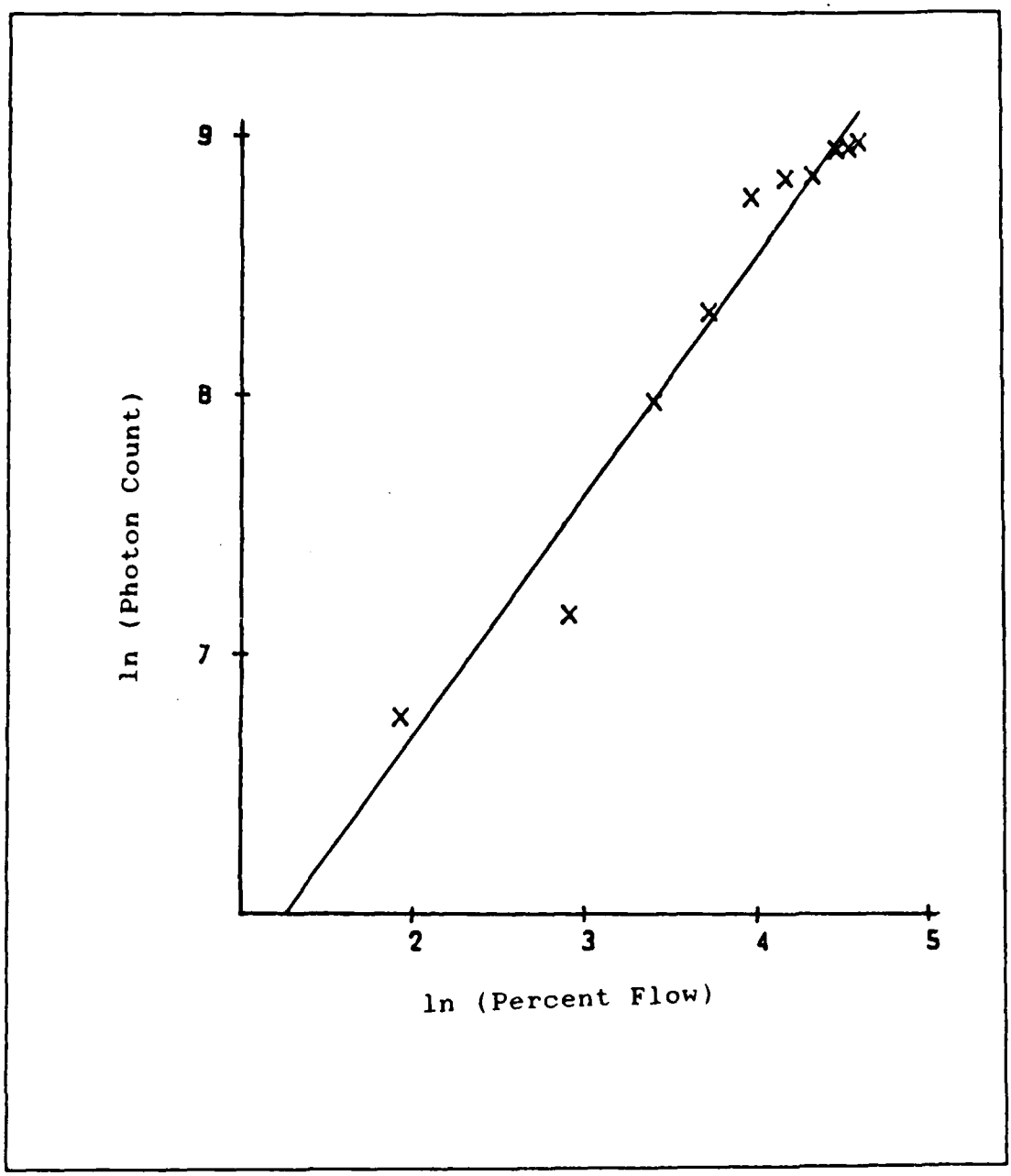

Figure 5.4. Graph of Flame Intensity as a Function of Percent Flow: Data Set Two

Data set one produced a linear slope of 0.80 and data set two produced a slope of 0.93. These slopes are both within experimental error of the proposed slope of 1.00. Several sets of data were taken, and the slope varied between 0.71 and 0.96.

Proposed reaction mechanism three involves a sequential reaction between an integer number of $O_2(^1\Delta)$ molecules and the IF molecule. Each oxygen molecule raises the IF molecule to a higher vibrational and rotational energy level within the ground electronic state. Although three ground vibrational O_2 molecules possess the correct amount of energy to align the IF(X) molecule with the IF(B) state, the kinetic analysis result does not depend on the number of sequential reactions. A slope of one is produced no matter how many two-body collisions take place to raise the ground state IF molecule to the IF(B) state.

In terms of probabilities, mechanism one, which is a four-body reaction, is the least likely especially considering the low pressure environment. Mechanisms two and three, which are both two-body collisions, have about the same chances of occurring. Since the data produced a slope very close to one, it appears that a sequential reaction within the IF ground electronic state is occurring.

In order to insure that there was a sufficient HgO coating on the oxygen inlet tube, the experiments were repeated just after a fresh HgO layer had been applied.

There was no apparent change in the data, which indicates that the atomic oxygen was being removed.

Although these results do not determine that mechanism three is the correct reaction, they do establish evidence in support of that proposition.

VI. Conclusions and Recommendations

Introduction

This section addresses the conclusions reached after performing this experiment and the recommendations for future work in this area.

Conclusions

A gas flow tube reactor has been used to generate a chemiluminescent flame from iodine monofluoride and excited oxygen in the singlet delta state, $O_2(^1\Delta)$. The flame has been optimized by varying the pressure, flow rate, and reactant proportions. Emission was observed, and the spectrum was compared with the known spectrum of IF(B$\longrightarrow$X).

The concentration of $O_2(^1\Delta)$ has been varied while keeping the total oxygen flow rate constant, and the intensity of the chemiluminescent flame has been measured.

The natural log of the intensity versus the natural log of the $O_2(^1\Delta)$ percent flow ($O_2(^1\Delta)$ concentration) have been graphed and a line has been fit to the data using linear regression analysis. The slope of the line varied between 0.71 and 0.96 over several data sets. This slope is well within experimental error of a slope of 1.00. It is found, on the basis of the results obtained, that the mechanism involving a sequential pumping of the IF molecules within the vibrational manifold by $O_2(^1\Delta)$ (mechanism three) is consistent with the experimental observations.

Recommendations

Vacuum Pump. A smaller valve should be added to the vacuum pump to allow more precise adjustments to be made in the flow rate. The present valve is very large and only coarse flow rate adjustments can be made.

Vibration Isolation. The vacuum pump should be mechanically isolated from the flow tube reactor because the vibrations cause the flow meters to bounce which reduces the measurement accuracy.

Improved Flow Metering. Although the flow meters used during this study were acceptable, meters covering several flow ranges would improve the measurement accuracy.

Vibrationally Excited IF. Vibrationally excited IF should be prepared using fluorine and iodine, and a study similar to this thesis should be performed. Vibrationally excited IF should be prepared by the following reaction:

$$F + I_2 \longrightarrow IF(X, v'' \geq 10)$$

Iodine-Oxygen Study. Iodine is another candidate for a chemical laser active medium. A flame intensity versus oxygen concentration study should be performed to better understand the pertinent reaction mechanisms. Iodine should be prepared by the following reaction:

$$I_2 + O_2(^1\Delta) \longrightarrow I$$

Carbon Dioxide Quenching. CO_2 gas should be added to the oxygen flow after the microwave cavity to quench $O_2(^1\Sigma)$. This modification to the system will help determine if mechanism two is a valid model because that model relies on the creation of $O_2(^1\Sigma)$. In addition, this experiment will rule out the possibility of $O_2(^1\Delta)$ generated in the discharge pumping vibrationally excited IF. If the data produces a slope of one after $O_2(^1\Sigma)$ is quenched by CO_2, then mechanism two can be ruled out.

Bibliography

1. Clyne, M. A. A. and I. S. McDermid. "$B^3\Pi(O^+)$ States of IF, ICl, and IBr," Journal of the Chemical Society Faraday Transactions II, 72: 2242-2251 (May 1976).

2. Davis, S. J. Potential of Halogen Molecules as Visible Chemical Laser Systems. Unpublished report No. AFWL-TR-79-104. Wright-Patterson AFB OH, 1979.

3. Davis, S. J. and others. Chemical Pump Sources for IF(B): Interim Report, 1 March 1986-10 July 1986. Contract F29601-86-C-0017. Kirtland AFB, NM: Air Force Weapons Laboratory, July 1986.

4. Davis, S. J. and others. Chemical Pump Sources for IF(B): Interim Report, 10 July 1986-10 October 1986. Contract F29601-86-C-0017. Kirtland AFB, NM: Air Force Weapons Laboratory, November 1986.

5. Davis, S. J. and others. Chemical Pump Sources for IF(B): Interim Report, 10 October 1986-10 January 1987. Contract F29601-86-C-0017. Kirtland AFB, NM: Air Force Weapons Laboratory, February 1987.

6. Dorko, Ernest A., AF Weapons Laboratory. Personal Interviews. AFIT, Wright-Patterson AFB OH, 2 March through 30 March 1987.

7. Duray, Capt Jeffery P. Spectroscopic Studies of Lead Oxide in a Flow Tube. MS Thesis, AFIT/GEP/PH/84D-2. School of Engineering, Air Force Institute of Technology (AU), Wright-Patterson AFB OH, December 1984.

8. Herzberg, Gerhard. Spectra of Diatomic Molecules. New York: Van Nostrand Reinhold Company, 1950.

9. Herzberg, Gerhard. The Spectra and Structures of Simple Free Radicals. Ithaca New York: Cornell University Press, 1971.

10. Lowe, John P. Quantum Chemistry. New York: Academic Press, 1978.

11. Photomultiplier C31034. Product Literature. RCA, Electro Optics and Devices Division, Lancaster, PA 17604.

12. Ritchey, Capt Conrad M. Spectroscopy and Kinetics of Lead Oxide. MS Thesis, AFIT/GEP/PH/83D-10. School of Engineering, Air Force Institute of Technology (AU), Wright-Patterson AFB OH, December 1983.

13. Stein, L., J. Wanner, and H. Walther. "Laser-induced Fluorescence Study of the Reactions of F Atoms with CH_3I and CF_3I." Journal of Chemical Physics, 72: 1128-1137 (January 1980).

14. Steinfeld, J. I. Molecules and Radiation. Boston: The MIT Press, 1978.

15. Wasserman, H. H. and R. W. Murray. Singlet Oxygen. New York: Academic Press, 1979.

16. Whitefield, P. D., R. F. Shea, and S. J. Davis. "Singlet Molecular Oxygen Pumping of IF(B)," Journal of Chemical Physics, 78: 6793-6801 (June 1983).

17. Wolf, Capt Paul J. Collisional Dynamics of the $B^3\Pi(0^+)$ State of Iodine Monofluoride. PhD dissertation. School of Engineering, Air Force Institute of Technology (AU), Wright-Patterson AFB OH, December 1983.

Vita

Ray O. Johnson was born in Kansas City, Missouri on 25 May 1955. He enlisted in the United States Air Force on 13 February 1975. He graduated from Oklahoma State University in May 1984 with a degree of Bachelor of Science in Electrical Engineering. He joined Phi Kappa Phi, Tau Beta Pi, and Eta Kappa Nu honor societies. He received a commission in the Air Force from Officer Training School in August 1984, where he was an honor graduate. He was assigned to HQ Foreign Technology Division as a Foreign Telecommunications Analyst until entering the School of Engineering, Air Force Institute of Technology, in June 1986.

Next Assignment: HQ SAC/XPY
Offutt AFB, NE 68113

UNCLASSIFIED
SECURITY CLASSIFICATION OF THIS PAGE

AD-A189 801

REPORT DOCUMENTATION PAGE

Form Approved OMB No. 0704-0188

1a. REPORT SECURITY CLASSIFICATION: UNCLASSIFIED	1b. RESTRICTIVE MARKINGS
2a. SECURITY CLASSIFICATION AUTHORITY	3. DISTRIBUTION/AVAILABILITY OF REPORT: Approved for public release; distribution unlimited.
2b. DECLASSIFICATION/DOWNGRADING SCHEDULE	
4. PERFORMING ORGANIZATION REPORT NUMBER(S): AFIT/GE/ENG/87D-27	5. MONITORING ORGANIZATION REPORT NUMBER(S)
6a. NAME OF PERFORMING ORGANIZATION: School of Engineering; 6b. OFFICE SYMBOL (If applicable): AFIT/ENG	7a. NAME OF MONITORING ORGANIZATION
6c. ADDRESS (City, State, and ZIP Code): Air Force Institute of Technology, Wright-Patterson AFB, OH 45433-6583	7b. ADDRESS (City, State, and ZIP Code)
8a. NAME OF FUNDING/SPONSORING ORGANIZATION; 8b. OFFICE SYMBOL (If applicable)	9. PROCUREMENT INSTRUMENT IDENTIFICATION NUMBER
8c. ADDRESS (City, State, and ZIP Code)	10. SOURCE OF FUNDING NUMBERS: PROGRAM ELEMENT NO. / PROJECT NO. / TASK NO / WORK UNIT ACCESSION NO.

11. TITLE (Include Security Classification): See Box 19

12. PERSONAL AUTHOR(S): Ray C. Johnson, B.S., 1Lt, USAF

13a. TYPE OF REPORT	13b. TIME COVERED	14. DATE OF REPORT (Year, Month, Day)	15. PAGE COUNT
MS Thesis	FROM 6/87 TO 11/87	1987, ~~11, 30~~ Dec	66

16. SUPPLEMENTARY NOTATION

17. COSATI CODES			18. SUBJECT TERMS (Continue on reverse if necessary and identify by block number)
FIELD	GROUP	SUB-GROUP	
20	05		Singlet Delta Oxygen, Iodine Monofluoride, Spectroscopy, Chemical Laser, Kinetics, Chemiluminescence
07	05		

19. ABSTRACT (Continue on reverse if necessary and identify by block number)

Title: STUDY OF THE ENERGY TRANSFER MECHANISMS BETWEEN $O_2(^1\Delta)$ AND IODINE MONOFLUORIDE

Thesis Chairman: Won B. Roh
Professor of Engineering Physics

Approved for public release: IAW AFR 190-1
LYNN E. WOLAVER
Dean for Research and Professional Development
Air Force Institute of Technology (AU)
Wright-Patterson AFB OH 45433-6583
24 Dec 87

20. DISTRIBUTION/AVAILABILITY OF ABSTRACT	21. ABSTRACT SECURITY CLASSIFICATION
☐ UNCLASSIFIED/UNLIMITED ☒ SAME AS RPT. ☐ DTIC USERS	UNCLASSIFIED

22a. NAME OF RESPONSIBLE INDIVIDUAL	22b. TELEPHONE (Include Area Code)	22c. OFFICE SYMBOL
Won B. Roh	(513) 255-2012	AFIT/ENP

DD Form 1473, JUN 86 — Previous editions are obsolete.

SECURITY CLASSIFICATION OF THIS PAGE
UNCLASSIFIED

Chemiluminescence from the reaction between iodine monofluoride (IF) and oxygen has been observed in a flow tube reactor. Molecular oxygen in the singlet delta, first electronic excited state, $O_2(^1\Delta)$, has been used as the transfer agent. The IF(X⟶B) transition requires 19054 cm^{-1} of energy, and $O_2(^1\Delta)$ can only supply 7918 cm^{-1} of energy in the transition to the ground state, $O_2(^3\Sigma)$. Despite the energy imbalance, $O_2(^1\Delta)$ is an efficient pump for IF. The kinetic mechanisms for this reaction are not well understood. The spectrum obtained from this emission has been compared to a known IF(B⟶X) spectrum, and transitions have been assigned. A study of the emission intensity as a function of the $O_2(^1\Delta)$ concentration has been made. From the slope of the lines produced from the data, a possible reaction mechanism has been identified.

END
DATE
FILM
4-88
DTIC